Bioorganic Chemistry 90 (2019) 103102

Contents lists available at ScienceDirect

Bioorganic Chemistry

journal homepage: www.elsevier.com/locate/bioorg

Synthesis, biological evaluation and *in silico* studies with 4-benzylidene-2-phenyl-5(4*H*)-imidazolone-based benzenesulfonamides as novel selective carbonic anhydrase IX inhibitors endowed with anticancer activity

Wagdy M. Eldehna[a,*], Mohamed A. Abdelrahman[b], Alessio Nocentini[c,d], Silvia Bua[c], Sara T. Al-Rashood[e], Ghada S. Hassan[f], Alessandro Bonardi[c,d], Abdulrahman A. Almehizia[e], Hamad M. Alkahtani[e], Amal Alharbi[e], Paola Gratteri[d], Claudiu T. Supuran[c,*]

[a] Department of Pharmaceutical Chemistry, Faculty of Pharmacy, Kafrelsheikh University, Kafrelsheikh, Egypt
[b] Department of Pharmaceutical Chemistry, Faculty of Pharmacy, Egyptian Russian University, Badr City, Cairo 11829, Egypt
[c] Department of NEUROFARBA, Section of Pharmaceutical and Nutraceutical Sciences, University of Florence, Polo Scientifico, Via U. Schiff 6, 50019, Sesto Fiorentino, Firenze, Italy
[d] Department of NEUROFARBA, Section of Pharmaceutical and Nutraceutical Sciences, Laboratory of Molecular Modeling Cheminformatics & QSAR, University of Florence, Polo Scientifico, Via U. Schiff 6, 50019, Sesto Fiorentino, Firenze, Italy
[e] Department of Pharmaceutical Chemistry, College of Pharmacy, King Saud University, P.O. Box 2457, Riyadh 11451, Saudi Arabia
[f] Department of Medicinal Chemistry, Faculty of Pharmacy, Mansoura University, Mansoura 35516, Egypt

ARTICLE INFO

Keywords:
Anticancer activity
Benzenesulfonamides
Imidazolone
Molecular modeling
Selective hCA IX inhibitors

ABSTRACT

In the presented work, we report the synthesis of a series of 4-benzylidene-2-phenyl-5(4*H*)-imidazolone-based benzenesulfonamides **7a-f** *via* the Erlenmeyer–Plöchl reaction. All the prepared imidazolones **7a-f** were evaluated as inhibitors of human (h) carbonic anhydrases (CA, EC 4.2.1.1) cytosolic isoforms hCA I and II, as well as transmembrane tumor-associated isoforms hCA IX and XII. All the tested hCA isoforms were inhibited by the prepared imidazolones **7a-f** in variable degrees with the following K_Is ranges: 673.2–8169 nM for hCA I, 61.2–592.1 nM for hCA II, 23–155.4 nM for hCA XI, and 21.8–179.6 nM for hCA XII. In particular, imidazolones **7a**, **7e**, and **7f** exhibited good selectivity towards the tumor-associated isoforms (CAs IX and XII) over the off-target cytosolic (CAs I and II) with selectivity index (SI) in the range of 6.2–19.4 and 3.3–8, respectively. Moreover, imidazolones **7a-f** were screened for their anticancer activity in one dose (10^{-5} M) assay against a panel of 60 cancer cell lines according to US-NCI protocol. Furthermore, **7a, 7e** and **7f** were evaluated for their anti-proliferative activity against colorectal cancer HCT-116 and breast cancer MCF-7 cell lines. Furthermore, **7e** and **7f** were screened for cell cycle disturbance and apoptosis induction in HCT-116 cells. Finally, a molecular docking study was carried out to rationalize the obtained results.

1. Introduction

Carbonic anhydrases (CA, EC 4.2.1.1) are a group of zinc containing metalloenzymes and are vastly distributed in living organisms. CAs are distributed into seven classes, α, β, γ, δ, ζ, η and θ. The hydration of carbon dioxide to produce bicarbonate and protons catalysed by the CAs have critical role in various human physiological processes such as respiration, pH and CO2 homeostasis, lipogenesis, gluconeogenesis and tumorigenicity [1]. The human carbonic anhydrases (hCAs) belong to the α- class of carbonic anhydrases. This family of CA is divided into fifteen isoforms, which exhibit distinct molecular attributes, protein structure, kinetics, localization and catalytic behaviour [2,3]. The isoforms can be listed as: CA I, CA II, CA III, CA VII and CA XIII are cytosolic, CA IV, CA IX, CA XII, and CA XIV are transmembrane bound, CA VA and VB mitochondrial and CA VI secreted in body fluids like saliva and colostrum [4–8].

CAs IX and XII are well-known transmembrane CA isoforms which have shown increased expression in hypoxia-induced tumor cells [9]. Human CA IX plays a great role in tumor cell proliferation, pH regulation migration and adhesion, thus the inhibition of hCA IX activity lead to a decrease of these processes and metastatic cascade [10]. Selective targeting of membrane-bound isoform hCA IX has been advised as a promising strategy to halt the growth of different solid tumours through suppressing distinctive tumour survival mechanisms in hypoxic

* Corresponding authors.
E-mail addresses: wagdy2000@gmail.com, wagdy.mohamad@pharm.kfs.edu.eg (W.M. Eldehna), claudiu.supuran@unifi.it (C.T. Supuran).

https://doi.org/10.1016/j.bioorg.2019.103102
Received 2 May 2019; Received in revised form 13 June 2019; Accepted 1 July 2019
Available online 02 July 2019
0045-2068/

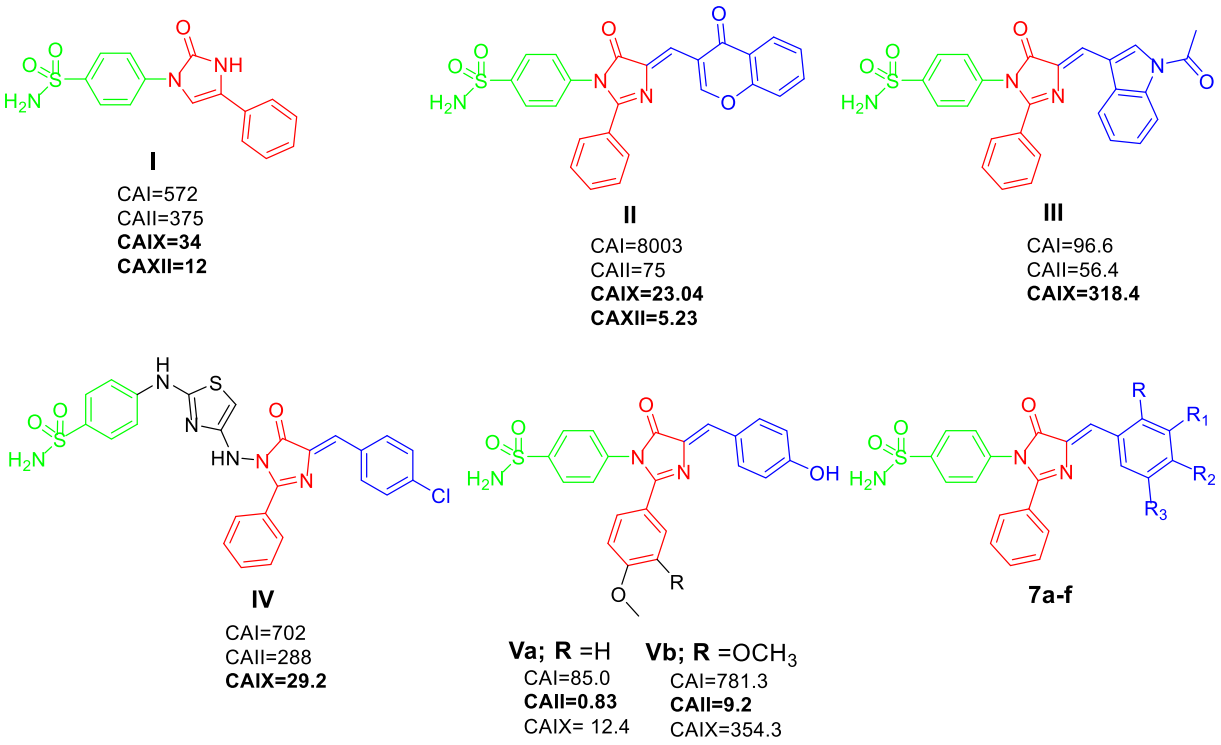

Fig. 1. Structures of some reported imidazolone-based benzenesulfonamides **I-V** and the target imidazolones **7a-f**.

environment [9,10]. A leading pre-clinical proof-of-concept data and one front-runner small molecule, SLC-0111, in Phase I/II clinical trials for the treatment of advanced hypoxic tumours [11,12] provides confidence that selective targeting of hCA isoforms will guarantee clinical validation in the near future.

In the last few years, aryl imidazolone scaffold have attracted attention as an effective and promising scaffold for the design and development of potent CA inhibitors. Congiu et al. [13] reported the synthesis and biological evaluation of novel 4-phenyl-imidazol-2(3*H*)-one derivatives as CA inhibitors (e.g. compound **I** in Fig. 1). These imidazol-2-ones emerged as selective nanomolar CAs IX and XII inhibitors.

Awadallah and co-workers reported two studies about the development of novel imidazolone-based benzenesulfonamides as CA inhibitors [14,15]. In the first study, the 2-phenyl-imidazol-5(1*H*)-one scaffold was condensed with a chromone moiety, (e.g. compound **II** in Fig. 1), whereas in the second study the 2-phenyl-imidazol-5(1*H*)-one scaffold was condensed with an indole moiety (e.g. compound **III** in Fig. 1). Uniquely the imidazolone-chromone hybrids (compound **II,** Fig. 1) exhibited good activity and selectivity towards the tumor-associated isoforms hCA IX and XII. Accordingly, they were evaluated for their anti-proliferative and pro-apoptotic activities towards cancer MCF-7 and A-549 cell lines. In 2016, another study [16] explored the synthesis and biological evaluation of novel CA inhibitors based on the 2-phenyl-imidazol-5(1*H*)-one scaffold (e.g. compound **IV** in Fig. 1), hinting that grafting a benzylidene moiety at imidazolone C-4 is well tolerated rather than the heteroaryl chromone moiety, and could result in more effective CA IX inhibitors.

Latterly, the Supuran's research group reported a new series of 1,2,4-trisubstituted imidazolin-5-ones bearing a 4-benzylidene moiety, and incorporating primary and secondary sulfonamide groups as dual carbonic anhydrase (isoforms I, II, IV and IX) and p38-MAPK inhibitors (e.g. compounds **Va and Vb** in Fig. 1) [17]. The SAR outcomes in this study revealed that presence of the free primary sulfamoyl group is crucial for the CA inhibitory activity. Conversely, it is noteworthy that incorporation of di-substituted phenyl moiety at C-2 (3,4-dimethoxy) elicited a worsening of effectiveness towards isoform hCA IX, suggesting that decreasing bulkiness of the substituent at C-2 of the imidazolone moiety is more advantageous for CA IX inhibitory activity (e.g. compounds **Va and Vb** in Fig. 1). Unfortunately, the four prepared primary sulfonamides reported in this study exhibited a high selectivity towards the off-target cytosolic isoform CA II over the tumor-associated isoform CA IX with IX/II selectivity indexes (SIs) spanning in the range of 10 – 175, though they displayed good to moderate CA IX inhibitory activity (K_Is values ranging between 12.4 and 902.4 nM).

Encouraged by the facts mentioned above and mindful of the significance of continuous development of selective hCA IX inhibitors to feed into anticancer discovery pipeline, we pursued on our efforts [18–20] to develop effective antitumor candidates that selectively targeting the tumor-associated isoform hCA IX. In the presented work, we report the synthesis of 4-benzylidene-2-phenyl-5(4*H*)-imidazolone-based benzenesulfonamides **7a-f** *via* the Erlenmeyer–Plöchl reaction (Fig. 1). Firstly, unsubstituted phenyl group (as in compounds **II-IV**) was selected to substitute the C-2 of the imidazolone core. Also, different un/substituted benzylidene derivatives were grafted at imidazolone C-4. The substitution pattern on the pendant 4-benzylidene moieties was selected to ensure diverse lipophilic and electronic environments that would manipulate the CA inhibitory activity of the target imidazolones. All the synthesized imidazolones **7a-f** were characterized and biologically tested against the physiologically relevant hCA isoforms, hCA I, II (cytosolic) as well as hCA IX and XII (transmembrane, tumor-associated isoforms) using stopped-flow CO_2 hydrase assay. As no attention was paid to investigate the potential binding mode of the reported imidazolone-based sulfonamides (compounds I-V, Fig. 1 [13–17]) within CAs active sites to understand how they can inhibit CAs, a molecular docking study for the prepared imidazolones within CA II and IX active sites was carried out to rationalize the obtained results.

Moreover, imidazolones **7a-f** were screened for their anticancer activity with one dose (concentration 10^{-5} M) assay towards a panel of 60 cancer cell lines according to US-NCI protocol. Furthermore, the most potent and selective hCA IX inhibitors were assessed for their anti-proliferative activity towards breast cancer MCF-7 and colorectal cancer HCT-116 cell lines. Then, imidazolones **7e** and **7f** were

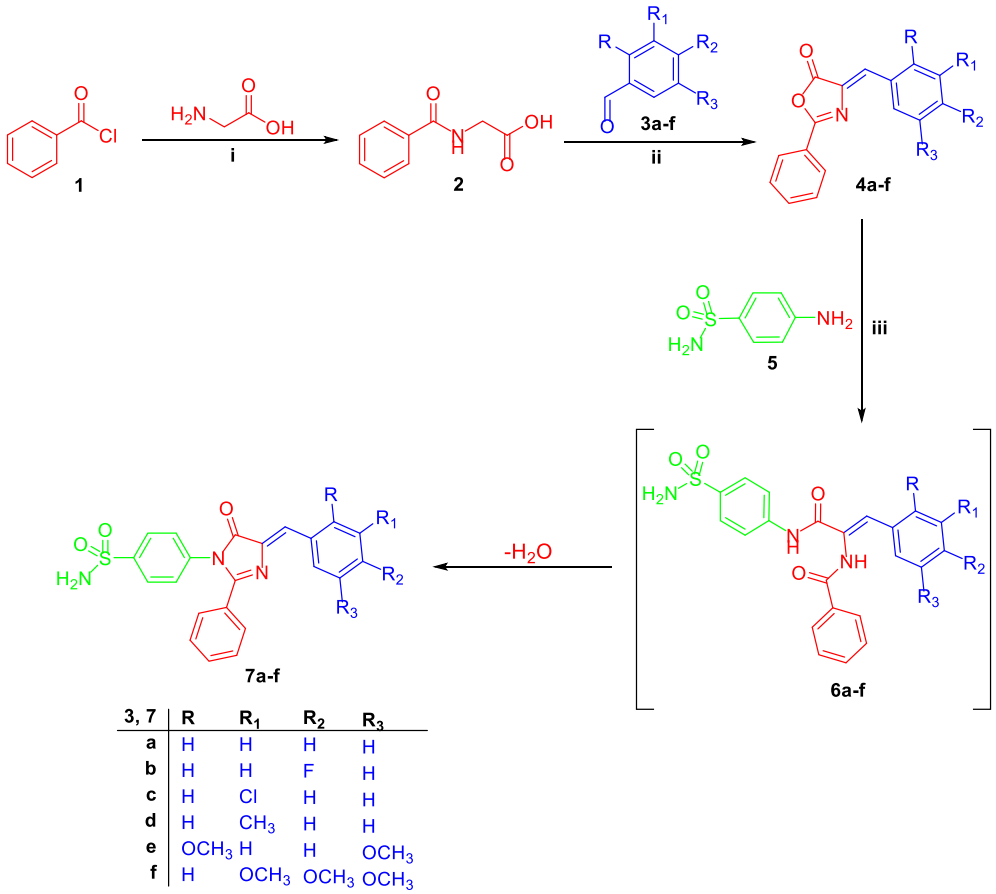

3, 7	R	R_1	R_2	R_3
a	H	H	H	H
b	H	H	F	H
c	H	Cl	H	H
d	H	CH_3	H	H
e	OCH_3	H	H	OCH_3
f	H	OCH_3	OCH_3	OCH_3

Scheme 1. Synthesis of imidazolone-based benzenesulfonamides **7a-f**; *Reagents and conditions*: (**i**) Aq. NaOH, r.t. 2 hrs., (**ii**) Acetic anhydride/Hünig's base/reflux 3 hrs., (**iii**) Glacial acetic acid/CH_3COONa/reflux 4 hrs.

examined for cell cycle disturbance and apoptosis induction in colorectal cancer HCT-116 cells to acquire more mechanistic insights into their antitumor activity.

2. Results and discussion

2.1. Chemistry

The synthetic strategy for the synthesis of the target imidazolone-based benzenesulfonamides **7a-f** was illustrated in Scheme 1. The synthesis was started by preparation of *N*-benzoylglycine (hippuric acid, **2**) *via N*-acylation of glycine with benzoyl chloride **1** as reported [21]. The key intermediates **4a-f** were prepared through the Erlenmeyer–Plöchl azlactone synthesis [22,23]; where hippuric acid **2** was reacted with different benzaldehydes **3a-f** in acetic anhydride in the presence of Hünig's base [24]. The key intermediates **4a-f** were refluxed with sulfanilamide **5** in glacial acetic acid and fused sodium acetate to furnish imidazolone-based benzenesulfonamides **7a-f** with 68–77% yield (Scheme 1).

Postulated structures of the prepared imidazolone-based benzenesulfonamides **7a-f** were in full agreement with their spectral and elemental analyses data.

IR spectra of sulfonamides **7a-f** revealed the presence of characteristic bands of NH_2 group (at 3316 – 3249 cm^{-1}), C=O group (at 1636 – 1629 cm^{-1}), and SO_2 at (1358 – 1350 and 1186–1157 cm^{-1}). Furthermore, ^1H NMR spectra of imidazolones **7a-f** displayed one D_2O exchangeable singlet signal assigned to (NH_2) of sulfonamido group at δ 7.40–7.50 ppm. In addition, compounds **7a-f** were confirmed by presence of olifenic signal at δ 7.25–7.39 ppm, whereas, ^1H NMR spectra of **7d, e** and **f** confirmed the presence of aliphatic signals of CH_3 at δ 1.84 ppm, two OCH_3 at δ 3.77–3.86 ppm and three OCH_3 at δ 3.74–3.84 ppm, respectively.

On the other hand, ^{13}C NMR spectra of imidazolones **7a-f** revealed presence of signal of (C=O) group at δ 169.65–169.81 ppm, in addition to, aliphatic CH_3 signals of **7d** at δ 21.48 ppm and OCH_3 signals of **7e,f** at δ 55.84–60.69 ppm.

2.2. Biological evaluation

2.2.1. Carbonic anhydrase inhibition

The CA inhibitory effects of all the synthesized imidazolone-based benzenesulfonamides **7a-f** were evaluated towards the physiologically relevant hCA isoforms, hCA I, II (cytosolic) as well as hCA IX and XII (transmembrane, tumor-associated isoforms) using an applied photophysics stopped-flow instrument for assaying the CA-catalyzed CO_2 hydration activity [25]. The inhibitory activities were compared to acetazolamide (AAZ), a clinically used standard CA inhibitor. The following SAR is evident from the data of Table 1:

i. The ubiquitous cytosolic isoform hCA I was inhibited by imidazolone-based benzenesulfonamides **7a-f** prepared in this study, with inhibition constants (K_Is) ranging from high nanomolar to low micromolar concentration, between 673.2 nM and 8.17 µM. Incorporation of unsubstituted benzylidene moiety led to sulfonamide **7a** with moderate inhibitory activity against hCA I (K_I = 692 nM). Since fluorine atom has a size and electronic properties similar to those of hydrogen, it was introduced as an isostere to the hydrogen atom. Sulfonamide **7b** bears fluorine substituent at the 4-position and showed mild improvement in the activity (K_I = 673.2 nM). On the other hand, grafting 3-Cl, 3-CH_3, 2,5-

Table 1
Inhibition data of human CA isoforms hCA I, II, IX and XII for imidazolone-based benzenesulfonamides **7a-f**, using (AAZ) as a standard drug.

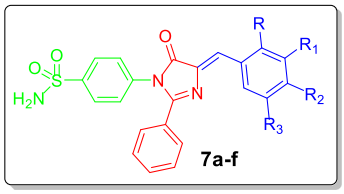

Comp.	R	R_1	R_2	R_3	K_I (nM)*			
					hCA I	hCA II	hCA IX	hCA XII
7a	H	H	H	H	692.0	362.7	58.7	76.5
7b	H	H	F	H	673.2	83.7	51.1	62.1
7c	H	Cl	H	H	823.1	61.2	155.4	21.8
7d	H	CH_3	H	H	4411.8	223.3	79.1	133.0
7e	OCH_3	H	H	OCH_3	8169.6	445.5	23.0	54.8
7f	H	OCH_3	OCH_3	OCH_3	5021.1	592.1	68.2	179.6
AAZ	–	–	–	–	250.0	12.0	25.0	5.7

* Mean from 3 different assays, by a stopped flow technique (errors were in the range of ± 5–10% of the reported values).

$(OCH_3)_2$ or 3,4,5-$(OCH_3)_3$ substituents at the benzylidene moiety (compounds **7c-f**; K_Is = 823.1, 4411.8, 8169.6 and 5021.1 nM, respectively) resulted in 1.2-, 6.4-, 11.8- and 7.3-fold decreased activity in comparison to their unsubstituted analogue **7a** (K_I = 692 nM).

ii. The second physiologically dominant isoform examined here was hCA II. It was evident from the obtained results that the prepared imidazolones **7a–f** exhibited inhibition constants ranging in the low-high nanomolar range, in detail, between 61.2 and 592.1 nM. Imidazolones **7b** and **7c** bearing 4-F and 3-Cl substituents, respectively, were the most potent hCA II inhibitors that displayed better activity (K_Is = 83.7 and 61.2 nM, respectively) than their unsubstituted counterpart **7a** (K_I = 362.7 nM), whereas, incorporation of 3-CH_3 substituent led to sulfonamide **7d** that displayed slight improvement in the inhibitory activity (K_I = 223.3 nM) than **7a**, suggesting that substitution with halogens is more advantageous than methyl group for hCA II inhibitory activity.

Similarly to the SAR for hCA I inhibition, incorporation of 2,5-$(OCH_3)_2$ or 3,4,5-$(OCH_3)_3$ substituents (compounds **7e, f**; K_Is = 445.5 and 592.1 nM, respectively) led to a decreased inhibitory activity in comparison to unsubstituted member **7a** (K_I = 362.7 nM).

iii. The *in vitro* kinetic data in Table 1 revealed that the tumor-associated isoform hCA IX was efficiently inhibited by the prepared imidazolone-based benzenesulfonamides **7a-f** with K_Is spanning in the nanomolar range: 23–79.1 nM, apart from imidazolone **7c** which possessed a slightly reduced inhibitory efficacy (K_I = 155.4 nM). Nevertheless, among the examined imidazolones, compound **7e** proved to be the most active one in inhibiting hCA IX in this study with K_I value of 23 nM, which is more potent than the standard drug AAZ (K_I = 25 nM). Concerning the effect of substitution of the benzylidene moiety, the hCA IX inhibitory activities were decreased in the order of 2,5-$(OCH_3)_2$ > 4-F > 3,4,5-$(OCH_3)_3$ > 3-CH_3 > 3-Cl.

iv. The second tumor-associated transmembrane isoform investigated here, hCA XII, was effectively inhibited by all the synthesized imidazolones **7a-f**, with K_Is in the range of 21.8–179.6 nM. In particular, imidazolone **7c** was the most potent hCA XII inhibitor (K_I = 21.8 nM). The decreased K_I values of the halogenated derivatives (compounds **7b** and **7c**; K_Is = 62.1 and 21.8 nM, respectively) than their unsubstituted counterpart **7a** (K_I = 76.5 nM), highlighted that incorporation of halogens within the benzylidene moiety is beneficial for the hCA XII inhibitory activity, as it was noticed for hCA II activity. On the contrary, substitution of the benzylidene moiety with 3-CH_3 or 3,4,5-$(OCH_3)_3$ groups decreased the activity (compounds **7d** and **7f**; K_Is = 133 and 179.6 nM, respectively). The order of activities for the substituted imidazolone-based benzenesulfonamides towards hCA XII was decreased in the order of 3-Cl > 2,5-$(OCH_3)_2$ > 4-F > 3-CH_3 > 3,4,5-$(OCH_3)_3$.

Table 2
Selectivity ratios for the inhibition of hCA IX and XII over hCA I and II for imidazolone-based benzenesulfonamides **7a-f** and acetazolamide.

Cmpd	I/IX	II/IX	I/XII	II/XII
7a	11.8	6.2	9	4.7
7b	13.2	1.6	10.8	1.3
7c	5.3	0.4	37.8	2.8
7d	55.8	2.8	33.2	1.7
7e	355	19.4	149.1	8
7f	73.6	8.7	28	3.3
AAZ	10.0	0.5	43.9	2.2

v. As a result of the profiles for inhibitory activities of the prepared imidazolone-based benzenesulfonamides **7a-f** (Table 1), the SI for each imidazolone-based benzenesulfonamide was calculated and listed in Table 2. Concerning selectivity towards hCA IX and XII over hCA I, all the evaluated imidazolones displayed excellent SIs spanning in the range of 5.3 – 73.6 and 9 – 149.1, respectively. Otherwise, only imidazolones **7a**, **7e**, and **7f** exhibited good selectivity towards hCA IX and XII over hCA II with SIs in the range of 6.2 – 19.4 and 3.3 – 8, respectively.

Of particular interest, substitution of the benzylidene moiety with 2,5-$(OCH_3)_2$ group, imidazolone **7e**, not only resulted in an enhancement of the inhibitory activity against hCA IX and XII, but also led to an worsening of effectiveness towards hCA I and II, in comparison to unsubstituted analogue **7a**. Such trend for **7e** resulted in the best selectivity profile for inhibition of the tumor-associated isoforms hCAs IX and XII over the off-target cytosolic hCAs I and II in this study (I/IX = 355, II/IX = 19.4, I/XII = 149.1 and II/XII = 8).

2.2.2. In vitro antitumor activity towards 60 cancer cell lines (NCI, USA)

The structures of all the prepared sulfonamides **7a-f** were submitted to the National Cancer Institute (NCI) Developmental Therapeutic Program (www.dtp.nci.nih.gov), where they were chosen to be *in vitro* evaluated for their antitumor activity. The selected sulfonamides were examined at single dose (10^{-5} M) primary anticancer assay towards a panel includes eighty five cancer lines. A 48 h drug exposure protocol was adopted, and sulforhodamine B (SRB) assay [26–28] was utilized to evaluate the cell growth and cell viability. The obtained data were reported as mean-graph of the percentage growth of the different treated cancer cells and showed as percentage growth inhibition (GI%) caused by the tested sulfonamides (Table 3). Exploration of results in Table 3 confirmed that the examined imidazolone-based benzenesulfonamides exhibited distinctive patterns of sensitivity and selectivity towards the different NCI cancer cell panels.

Close examination of the GI% values in Table 3, highlighted that imidazolone-based benzenesulfonamides **7a**, **7e** and **7f** were the most active anti-proliferative analogues in this study with broad spectrum activity against numerous cancer cell lines that belong to different tumor subpanels. The most susceptible cancer cell lines towards the impact of benzenesulfonamides **7a**, **7e** and **7f** were displayed in Fig. 2.

Imidazolone **7a** displayed broad spectrum activity towards forty one cancer cell lines represent all subpanels except leukemia. In particular, imidazolone **7a** exhibited a potent growth inhibitory activity against non-small cell lung cancer (A549 and HOP-62), colon cancer (HCT-116), CNS cancer (SNB-75), ovarian cancer (OVCAR-4 and OVCAR-8), renal cancer (ACHN) and breast cancer (MCF7) cell lines with

Table 3
Percentage growth inhibition (GI %) of *in vitro* subpanel tumor cell lines at 10 μM concentration for sulfonamides **7a-f**.

Subpanel/Cell line		Compound [a]					
		7a	**7b**	**7c**	**7d**	**7e**	**7f**
Leukemia	CCRF-CEM	–	–	16	–	10	–
	HL-60(TB)	–	10	18	–	–	–
	K-562	–	13	29	10	15	–
	MOLT-4	–	–	35	10	29	–
	RPMI-8226	–	–	–	–	20	10
	SR	–	30	68	31	20	38
Non-Small Cell Lung Cancer	A549/ATCC	41	22	22	25	16	10
	EKVX	–	–	–	–	–	–
	HOP-62	44	–	12	17	–	36
	HOP-92	12	–	–	–	23	28
	NCI-H226	13	–	–	–	–	16
	NCI-H23	18	–	–	11	10	–
	NCI-H322M	15	–	–	–	–	–
	NCI-H460	23	–	–	–	–	16
	NCI-H522	13	17	27	18	22	23
Colon Cancer	COLO 205	–	–	–	–	–	–
	HCC-2998	–	–	–	–	–	–
	HCT-116	50	10	13	17	21	18
	HCT-15	15	20	25	–	14	10
	HT29	14	–	22	14	–	–
	KM12	11	–	12	–	–	–
	SW-620	–	–	–	–	–	–
CNS Cancer	SF-268	22	–	–	–	10	19
	SF-295	23	–	–	14	11	24
	SF-539	34	13	–	28	10	22
	SNB-19	19	–	–	20	–	29
	SNB-75	73	10	17	51	26	61
	U251	31	–	–	–	15	–
Melanoma	LOX IMVI	–	–	–	–	11	–
	MALME-3M	13	–	13	18	–	20
	M14	–	–	–	–	–	–
	MDA-MB-435	12	–	14	–	–	–
	SK-MEL-2	–	–	–	–	–	–
	SK-MEL-28	–	–	–	–	–	–
	SK-MEL-5	10	–	–	12	17	–
	UACC-257	24	–	–	–	–	29
	UACC-62	13	–	14	–	27	16
Ovarian Cancer	IGROV1	11	–	–	–	46	13
	OVCAR-3	–	–	–	–	–	11
	OVCAR-4	47	–	30	23	18	43
	OVCAR-5	–	–	–	–	–	–
	OVCAR-8	42	12	21	27	11	54
	NCI/ADR-RES	21	–	15	12	16	–
	SK-OV-3	10	–	–	–	–	18
Renal Cancer	786–0	14	23	–	–	–	–
	A498	–	12	–	–	–	–
	ACHN	44	–	11	14	15	24
	CAKI-1	33	25	17	14	24	33
	RXF 393	–	15	–	–	–	20
	SN12C	20	–	–	–	11	21
	TK-10	10	–	–	–	–	–
	UO-31	23	12	20	–	41	24
Prostate	PC-3	16	–	19	–	25	16
	DU-145	10	–	–	–	–	–
Breast Cancer	MCF7	45	12	28	18	29	29
	MDA-MB-231	15	–	–	–	–	15
	HS 578 T	32	14	10	24	20	65
	BT-549	–	39	NT[b]	NT[b]	NT[b]	NT[b]
	T-47D	13	–	27	15	25	11
	MDA-MB-468	27	–	–	–	–	15
Mean growth, %		**83**	**94**	**90**	**91**	**89**	**85**
Sensitive cell lines no.		**41**	**18**	**26**	**23**	**31**	**34**

[a] Only GI % higher than 10% are shown.

inhibition % 41, 44, 50, 73, 47, 42, 44 and 45, respectively. Moreover, **7a** showed GI more than 25% over CNS cancer (SF-539 and U251), renal cancer (CAKI-1) and breast cancer (HS 578T and MDA-MB-468) cell lines. Furthermore, imidazolone **7f** possessed anti-proliferative activity towards thirty four cancer cell lines (Table 3) representing all subpanels, with potent growth inhibitory impact against CNS cancer (SNB-75), ovarian cancer (OVCAR-4 and OVCAR-8) and breast cancer (HS 578T) cell lines with inhibition % equal 61, 43, 54 and 65, respectively. Also, imidazolone **7f** exerted anti-proliferative effect with GI more than 25% against leukemia (SR), non-small cell lung cancer (HOP-62 and HOP-92), CNS cancer (SNB-19), melanoma (UACC-257), renal cancer (CAKI-1) and breast cancer (MCF7) cell lines.

It is noteworthy that non-small cell lung cancer (A549 and NCI-H522), colon cancer (HCT-116), CNS cancer (SNB-75), ovarian cancer (OVCAR-8), renal cancer (CAKI-1) and breast cancer (MCF7 and HS 578T) cell lines were sensitive to all the tested midazolone-based benzenesulfonamides (**7a-f**) with GI% range of 10–41%,13–27%, 10–50%, 10–73%, 11–54%, 14–33%, 12–45% and 10–65%, respectively.

2.2.3. Anti-proliferative activity towards breast MCF-7 and colon HCT-116 cancer cell lines

Association of CA IX overexpression with poor prognosis in breast and colon cancers is well reported in the literature [29–31]. As imidazolones **7a**, **7e** and **7f** displayed good inhibitory activity towards tumor-associated hCA IX isoform, and good hCA II/IX selectivity, they were selected to be evaluated for their anti-proliferative activity against breast cancer MCF-7 and colon cancer HCT-116 cell lines using the MTT colorimetric assay as described by T. Mosmann [32]. Staurosporine was used in this assay as a reference antitumor drug. The results were presented as IC_{50} values which are the compounds concentrations needed to produce a 50% inhibition of cell growth after 48 h of incubation, compared to untreated control (Table 4).

From the displayed results in Table 4, it was obvious that HCT-116 cells is more sensitive to the influence of the examined imidazolones (**7a**, **7e** and **7f**) with IC_{50} values equal 13.51 ± 0.77, 4.37 ± 0.12 and 3.21 ± 0.16 μM, respectively. In particular, sulfonamide **7f** was the most potent one with better activity (IC_{50} = 3.21 ± 0.16 μM) than that of the reference drug Staurosporine (IC_{50} = 4.54 ± 0.17 μM).

Concerning activity towards breast cancer MCF-7 cells, imidazolones **7a** emerged as the most active one that exhibited potent anti-proliferative activity with IC_{50} value equals 7.63 ± 0.31 μM, which is better than that of the reference drug Staurosporine (IC_{50} = 10.41 ± 0.49 μM). Moreover, imidazolones **7e** and **7f** possessed moderate activity against MCF-7 cells with IC_{50} values equal 14.57 ± 0.66 and 16.28 ± 0.84 μM, respectively.

2.2.4. Cell cycle analysis

The effect of imidazolone-based benzenesulfonamides **7e** and **7f** on cell cycle progression was evaluated in colorectal HCT-116 cells after 24 h of treatment (Fig. 3). This impact was determined through a DNA flow cytometric assay; where colorectal HCT-116 cells were treated with imidazolones **7e** and **7f** at their IC_{50} concentrations (IC_{50} = 4.37 ± 0.12 and 3.21 ± 0.16 μM, respectively).

As displayed in Fig. 3, this flow cytometric assay outcomes revealed that exposure of colorectal HCT-116 cells to imidazolones **7e** and **7f** resulted in a significant increase in the percentage of cells at Sub-G_1 by 6- and 7.5-folds, respectively, with concurrent significant arrest in the G_2-M phase by 2.9- and 6.3-folds, respectively, compared to control. Both alteration of the Sub-G_1 phase and arrest of G_2-M phase are considered to be significant remarks for imidazolone-based benzenesulfonamides **7e** and **7f** to persuade apoptosis in colorectal HCT-116 cells.

2.2.5. Annexin V-FITC apoptosis assay

Annexin V-FITC/propidium iodide (AV/PI) dual staining assay was carried out to evaluate the impact of both imidazolones **7e** and **7f** on early and late apoptosis percentages in colorectal HCT-116 cells (Fig. 4).

This analysis suggested that treatment of HCT-116 cells with imidazolones **7e** and **7f** resulted in a significant increase in the percent of

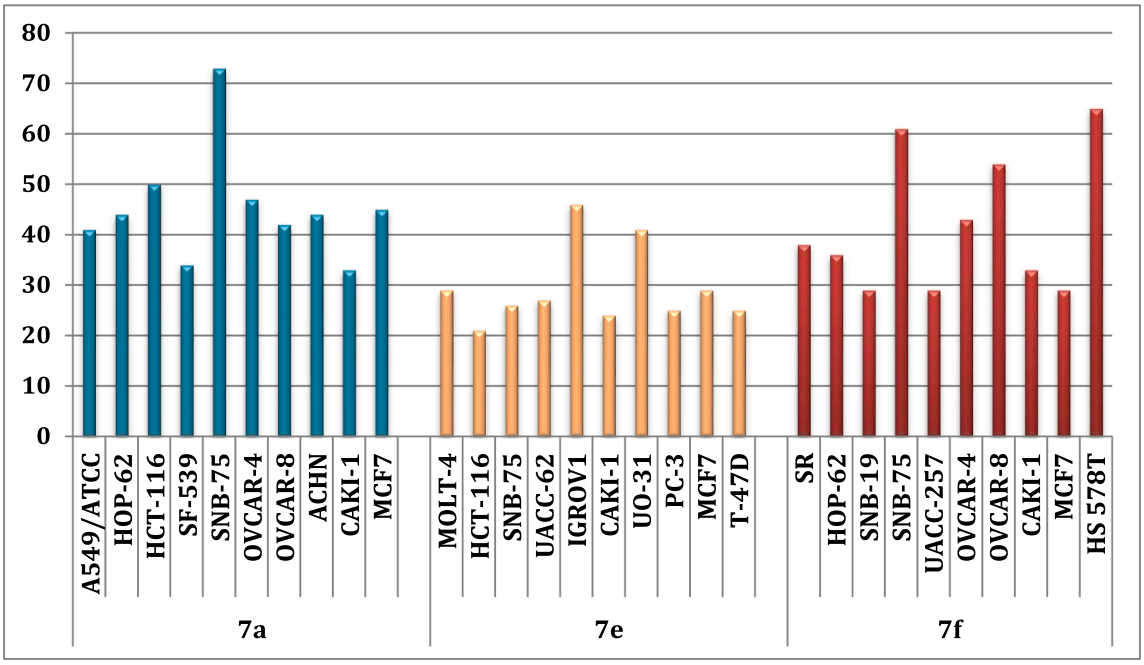

Fig. 2. The most susceptible NCI cancer cell lines towards the effect of target imidazolones **7a**, **7e** and **7f** according to the GI%.

Table 4
In vitro anti-proliferative activity of imidazolone-based benzenesulfonamides **7a**, **7e** and **7f** towards breast MCF-7 and colorectal HCT-116 cancer cell lines.

Comp.	IC_{50} (μM)[a]	
	MCF-7	HCT-116
7a	7.63 ± 0.31	13.51 ± 0.77
7e	14.57 ± 0.66	4.37 ± 0.12
7f	16.28 ± 0.84	3.21 ± 0.16
Staurosporine	10.41 ± 0.49	4.54 ± 0.17

[a] IC_{50} values are the mean ± S.D. of three separate experiments.

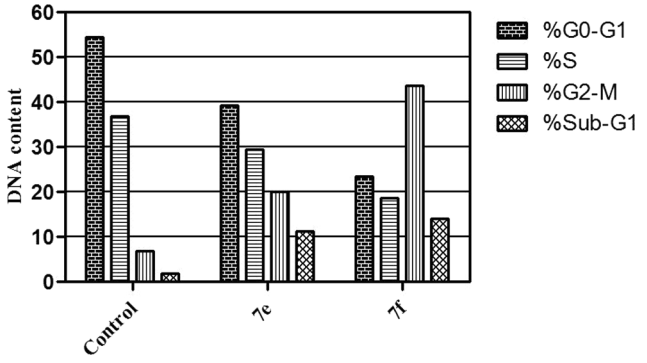

Fig. 3. Effect of imidazolone-based benzenesulfonamides **7e** and **7f** on the phases of cell cycle of HCT-116 cells.

annexin V-FITC-positive apoptotic cells, including both the early (from 0.95% to 5.09% for **7e**, and from 0.95% to 7.52% for **7f**) and late apoptotic (from 0.38% to 4.4% for compound **7e**, and from 0.38% to 6.21% for compound **7f**) phases (UR + LR), which represents about 7- and 10-folds total increase, respectively, as compared with the control.

2.3. Molecular modelling study

To point out the binding modes and to unveil the relationships between structural features and inhibition profile of the herein reported compounds, docking and MM-GBSA-based refinements within hCA isozymes II and IX (PDB 5LJT [33] and 5FL4 [34]) were performed. As expected, in all compounds docking solutions the benzenesulfonamide accommodates deeply into the active site region of both isozymes, with the negatively charged nitrogen of zinc-binding group coordinating the metal atom. Furthermore, H-bonds are formed by the NH^- group and T199 (N-H···OG1) and by the S═O and T199 (S = O···H-N), while the phenyl ring accommodates into an area defined by V121, V143 and L198. In hCA II, the heterocyclic ring is stabilized by contacts with F131, V135 and L198, whereas the unsubstituted phenyl ring of derivatives **7a-f**, placed in a small cleft defined by the hydrophilic residues N62, N67 and Q92, forms a π-π interaction with H64. The benzylidene moiety is oriented toward the exit of the active site, assuming different orientations according to the substituents decorating the ring (Fig. 5**A**).

In hCA IX, the carbonyl group of the heterocyclic ring of **7a-f** is in H-bond distance with T200 hydroxyl group, orienting the unsubstituted phenyl moiety towards a wide cleft lined by L91, Q92, V121, V131, L140. It is likely that the enhanced hCA IX vs II inhibition profile of the studied compounds derives from the better complementarity between the phenyl ring features and the hydrophobic residues present in the aforesaid pocket of the hCA IX active site. Again, the pendants of the benzylidene moiety determine the different orientations assumed by this ring in the outer area of the active site (Fig. 5**B**).

3. Conclusion

All the tested hCA isoforms were inhibited by the prepared imidazolones **7a-f** in variable degrees with the following K_Is ranges: 673.2–8169 nM for hCA I, 61.2–592.1 nM for hCA II, 23–155.4 nM for hCA XI, and 21.8–179.6 nM for hCA XII. Superiorly, imidazolone **7e** emerged as the most potent hCA IX inhibitor in this study with K_I value equals 23 nM, which is more potent than the standard drug AAZ (K_I = 25 nM). Regarding selectivity, imidazolones **7a**, **7e**, and **7f** exhibited good selectivity towards the tumor-associated isoforms (CAs IX & XII) over the off-target cytosolic (CAs I & II) with SIs in the range of 6.2–19.4 and 3.3–8, respectively. In particular, imidazolone **7e** displayed the best selectivity profile for isoforms hCAs IX and XII over hCAs I and II in this study (I/IX = 355, II/IX = 19.4, I/XII = 149.1 and II/XII = 8). On the other hand, imidazolones **7a-f** were screened for

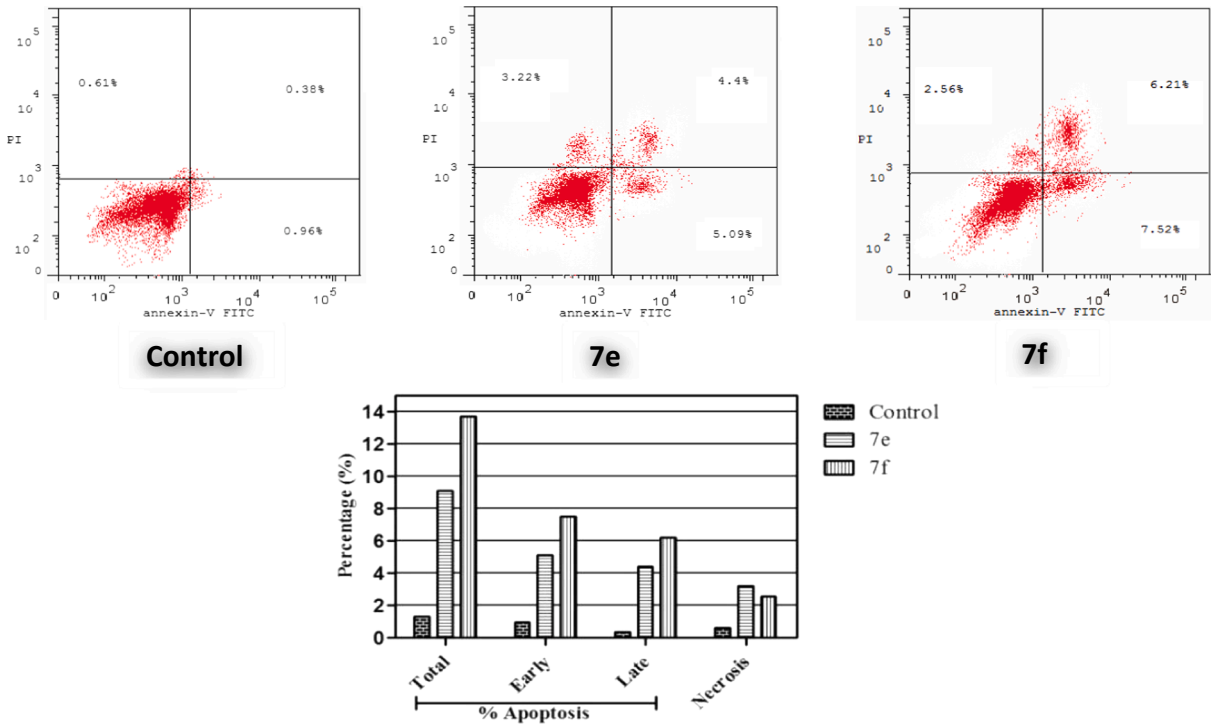

Fig. 4. Effect of imidazolone-based benzenesulfonamides **7e** and **7f** on the percentage of annexin V-FITC-positive staining in HCT-116 cells. The experiments were done in triplicates. The four quadrants identified as: **LL**, viable; **LR**, early apoptotic; **UR**, late apoptotic; **UL**, necrotic.

their anticancer activity at one dose (10^{-5} M) assay towards a panel of 60 cancer cell lines according to US-NCI protocol. Also, **7a, 7e** and **7f** were evaluated for their anti-proliferative activity against colorectal cancer HCT-116 and breast cancer MCF-7 cell lines. Imidazolones **7e** and **7f** possessed excellent activity against HCT-116 cells with IC_{50} values equal 4.37 ± 0.12 and 3.21 ± 0.16 μM, respectively. Accordingly, imidazolones **7e** and **7f** were screened for cell cycle disturbance and apoptosis induction in HCT-116 cells. They were found to persuade cell cycle arrest at G_2-M stage as well as alter the Sub-G_1 phase, in addition, they increased the percent of annexinV-FITC positive apoptotic cells from 1.33% to 9.13% for compound **7e**, and from 1.33% to 13.73% for compound **7f**. Finally, a molecular docking study for the prepared imidazolones within CA II and IX active sites was carried out (PDB; 5LJT and 5FL4, respectively) to rationalize the obtained results.

4. Experimental

4.1. Chemistry

4.1.1. General

Melting points were measured with a Stuart melting point apparatus and were uncorrected. The NMR spectra were recorded by Varian Gemini-400BB 400 MHz FT-NMR spectrometers (Varian Inc., Palo Alto, CA). ^{1}H and ^{13}C spectra were run at 400 and 100 MHz, respectively, in deuterated dimethylsulphoxide (DMSO-d_6). Chemical shifts (δ_H) are

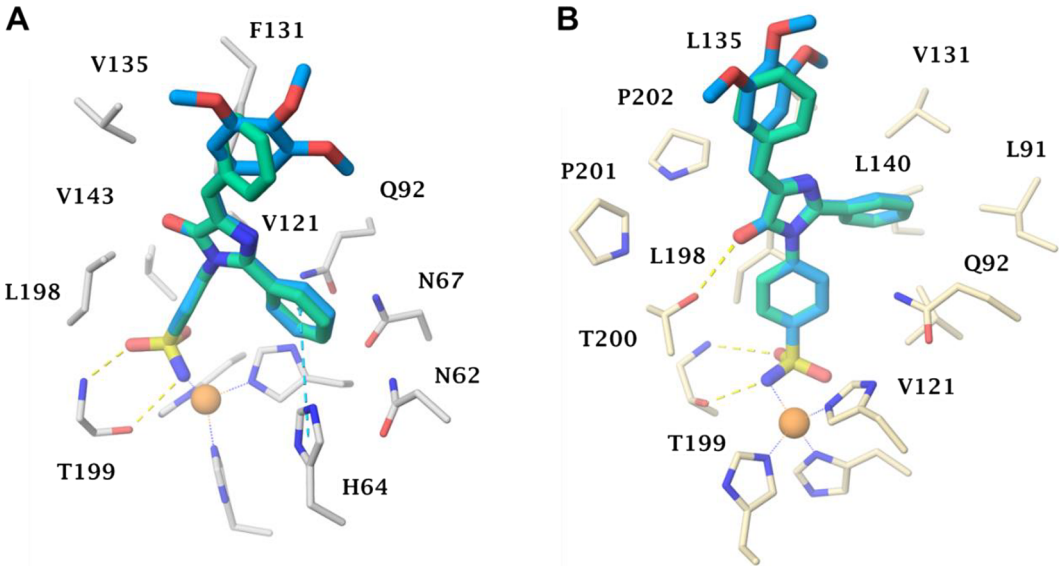

Fig. 5. Docking of **7a** (green) and **7f** (blue) in hCA II (**A**) and in hCA IX (**B**) active sites.

reported relative to TMS as internal standard. All coupling constant (*J*) values are given in hertz. Chemical shifts (δ_C) are reported relative to DMSO-d_6 as internal standards. The abbreviations used are as follows: s, singlet; d, doublet; m, multiplet. IR spectra were recorded with a Bruker FT-IR spectrophotometer. Reaction courses and product mixtures were routinely monitored by thin layer chromatography (TLC) on silica gel precoated F_{254} Merck plates. Unless otherwise noted, all solvents and reagents were commercially available and used without further purification. Compounds **4a-f** are previously reported [35,36].

*4.1.2. General procedure for preparation of target imidazolone-based benzenesulfonamides **7a-f***

A mixture of equimolar quantities of azlactone **4a-f** (2 mmol), sulfanilamide **5** (0.34 g, 2 mmol) and fused sodium acetate (0.16 g, 2 mmol) was refluxed in glacial acetic acid (5 mL) for 4 hrs. The precipitated solid was collected by filtration while hot, washed with cold methanol, dried and recrystallized from dioxan to furnish the corresponding imidazolone-based benzenesulfonamides **7a-f** with 68–77% yield.

*4.1.2.1. 4-(4-Benzylidene-5-oxo-2-phenyl-4,5-dihydro-1H-imidazol-1-yl) benzenesulfonamide (**7a**).* Yellow crystals (yield 77%), m.p. 211–213 °C; IR (KBr, ν cm^{-1}): 3316 (NH_2), 1705 (C═O) and 1350, 1168 (SO_2); ^{1}H NMR (DMSO-d_6) δ *ppm*: 7.30 (s, 1H, olefinic), 7.40–7.44 (m, 4H, Ar-H), 7.45–7.50 (m, 4H, Ar-H and D_2O exchangeable NH_2), 7.51–7.53 (m, 4H, Ar-H), 7.85 (d, 2H, J = 7.2 Hz, Ar-H), 8.34 (d, 2H, J = 7.2 Hz, Ar-H); ^{13}C NMR (DMSO-d_6) δ *ppm*: 127.15, 128.65, 128.91, 129.04, 129.38, 129.46, 131.18, 132.11, 132.88, 134.48, 137.71, 138.71, 144.14, 160.86, 169.81; Anal. calcd. for $C_{22}H_{17}N_3O_3S$ (403.46): C, 65.17; H, 4.25; N, 10.42. Found C, 65.01; H, 4.20; N, 10.38.

*4.1.2.2. 4-(4-(4-Fluorobenzylidene)-5-oxo-2-phenyl-4,5-dihydro-1H-imidazol-1-yl)benzenesulfonamide (**7b**).* Yellow crystals (yield 75%), m.p. 223–224 °C; IR (KBr, ν cm^{-1}): 3310 (NH_2), 1708 (C═O) and 1358, 1158 (SO_2); ^{1}H NMR (DMSO-d_6) δ *ppm*: 7.33–7.52 (m, 12H; 1H olefinic, 9H Ar-H and D_2O exchangeable NH_2), 7.85 (d, 2H, J = 8.4 Hz, Ar-H), 8.42–8.45 (m, 2H, Ar-H); ^{13}C NMR (DMSO-d_6) δ *ppm*: 116.42, 116.65, 127.13, 127.35, 128.62, 128.84, 129.01, 129.42, 131.19, 131.22, 132.10, 135.24, 135.33, 137.62, 138.29, 138.31, 144.15, 160.89, 160.91, 162.46, 164.95, 169.74; Anal. calcd. for $C_{22}H_{16}FN_3O_3S$ (421.45): C, 62.70; H, 3.83; N, 9.97. Found C, 62.42; H, 3.80; N, 10.03.

*4.1.2.3. 4-(4-(3-Chlorobenzylidene)-5-oxo-2-phenyl-4,5-dihydro-1H-imidazol-1-yl)benzenesulfonamide (**7c**).* White crystals (yield 70%), m.p. 250–252 °C; IR (KBr, ν cm^{-1}): 3313 (NH_2), 1701 (C═O) and 1350, 1168 (SO_2); ^{1}H NMR (DMSO-d_6) δ *ppm*: 7.31 (s, 1H, olefinic), 7.41–7.54 (m, 11*H*; 9H Ar-H and D_2O exchangeable NH_2), 7.85 (d, 2H, J = 8.4 Hz, Ar-H), 8.29 (d, 1H, J = 6.4 Hz, Ar-H), 8.44 (s, 1H, Ar-H); ^{13}C NMR (DMSO-d_6) δ *ppm*: 126.51, 127.14, 128.66, 128.72, 129.08, 129.47, 130.59, 131.17, 131.30, 131.81, 132.29, 133.93, 136.53, 137.52, 139.70, 144.19, 161.77, 169.65; Anal. calcd. for $C_{22}H_{16}ClN_3O_3S$ (437.90): C, 60.34; H, 3.68; N, 9.60. Found C, 60.55; H, 3.64; N, 9.53.

*4.1.2.4. 4-(4-(3-Methylbenzylidene)-5-oxo-2-phenyl-4,5-dihydro-1H-imidazol-1-yl)benzenesulfonamide (**7d**).* Yellow crystals (yield 68%), m.p. 259–261 °C; IR (KBr, ν cm^{-1}): 3312 (NH_2), 1703 (C═O) and 1353, 1165 (SO_2); ^{1}H NMR (DMSO-d_6) δ *ppm*: 2.38 (s, 3H, CH_3), 7.25 (s, 1H, olefinic), 7.27 (d, 2H, J = 8.0 Hz, Ar-H), 7.38 (d, 2H, J = 8.0 Hz, Ar-H), 7.42 (s, 2H, D_2O exchangeable NH_2), 744–7.53 (m, 5H, Ar-H), 7.85 (d, 2H, J = 7.2 Hz, Ar-H), 8.08 (s, 1H, Ar-H), 8.21 (d, 1H, J = 7.6 Hz, Ar-H); ^{13}C NMR (DMSO-d_6) δ *ppm*: 21.48 (CH_3), 127.12, 128.61, 128.80, 128.90, 129.02, 129.28, 129.41, 130.00, 131.94, 132.05, 133.44, 134.38, 137.69, 138.46, 138.55, 144.08, 160.67, 169.78; Anal. calcd. for $C_{23}H_{19}N_3O_3S$ (417.48): C, 66.17; H, 4.59; N, 10.07. Found C, 65.87; H, 4.63; N, 10.14.

*4.1.2.5. 4-(4-(2,5-Dimethoxybenzylidene)-5-oxo-2-phenyl-4,5-dihydro-1H-imidazol-1-yl)benzenesulfonamide (**7e**).* Orange crystals (yield 75%), m.p. 246–247 °C; IR (KBr, ν cm^{-1}): 3310 (NH_2), 1710 (C═O) and 1358, 1163 (SO_2); ^{1}H NMR (DMSO-d_6) δ *ppm*: 3.77 (s, 3H, OCH_3), 3.86 (s, 3H, OCH_3), 7.07–7.08 (m, 2H, Ar-H), 7.39–7.52 (m, 9H, Ar-H), 7.56 (s, 1H, Ar-H), 7.85 (d, 2H, J = 8.4 Hz, Ar-H), 8.55 (d, 1H, J = 1.6 Hz, Ar-H); ^{13}C NMR (DMSO-d_6) δ *ppm*: 55.84 (OCH_3), 56.74 (OCH_3), 113.05, 117.10, 118.91, 121.30, 123.15, 127.14, 128.61, 128.88, 129.07, 129.32, 132.10, 137.72, 138.18, 144.11, 153.46, 154.00, 160.46, 169.75; Anal. calcd. for $C_{24}H_{21}N_3O_5S$ (463.51): C, 62.19; H, 4.57; N, 9.07. Found C, 61.93; H, 4.60; N, 9.13.

*4.1.2.6. 4-(5-Oxo-2-phenyl-4-(3,4,5-trimethoxybenzylidene)-4,5-dihydro-1H-imidazol-1-yl)benzenesulfonamide (**7f**).* Orange crystals (yield 71%), m.p. 271–272 °C; IR (KBr, ν cm^{-1}): 3303 (NH_2), 1708 (C═O) and 1357, 1157 (SO_2); ^{1}H NMR (DMSO-d_6) δ *ppm*: 3.74 (s, 3H, OCH_3), 3.84 (s, 6H, 2 OCH_3), 7.26 (s, 1H, olefinic), 7.39–7.53 (m, 9H; 7H Ar-H and D_2O exchangeable NH_2), 7.82 (s, 2H, Ar-H), 7.86 (d, 2H, J = 8.8 Hz, Ar-H); ^{13}C NMR (DMSO-d_6) δ *ppm*: 56.37 (OCH_3), 60.69 (OCH_3), 110.58, 127.13, 128.59, 128.85, 128.92, 129.08, 29.27, 129.90, 132.06, 137.77, 137.78, 140.52, 144.10, 153.28, 159.99, 169.71; Anal. calcd. for $C_{25}H_{23}N_3O_6S$ (493.53): C, 60.84; H, 4.70; N, 8.51. Found C, 61.05; H, 4.68; N, 8.42.

4.2. Biological evaluation

4.2.1. CA inhibitory assay

An Applied Photophysics stopped-flow instrument has been used for assaying the CA catalysed CO_2 hydration activity, as reported earlier [25]. The inhibition constants were obtained by non-linear least-squares methods using PRISM 3 and the Cheng-Prusoff equation as reported earlier, and represent the mean from at least three different determinations. The four tested CA isofoms were recombinant ones obtained in-house as reported earlier [37–41].

4.2.2. In vitro antitumor activity towards 60 cancer cell lines

The antitumor assay was performed according to the protocol of the Drug Evaluation Branch, NCI, Bethesda [42–44]. A 48 h drug exposure protocol was adopted, and sulforhodamine B (SRB) assay [26] was utilized to assess the cell growth and viability, as reported earlier [45,46].

4.2.3. Antiproliferative activity against MCF-7 and HCT-116 cell lines

Breast cancer MCF-7 and colorectal cancer HCT-116 cell lines were obtained from American Type Culture Collection (ATCC). MCF-7 cells were grown in RPMI-1640 while HCT-116 cells were grown in DMEM. The cells were supplemented with 10% heat-inactivated fetal bovine serum, 1% L-glutamine (2.5 mM), HEPES buffer (10 mM), 50 µg/mL gentamycin. All cells were maintained at 37 C in a humidified atmosphere with 5% CO_2. Cytotoxicity was determined following the MTT assay, as reported earlier [47,48].

4.2.4. Cell cycle analysis

Colorectal HCT-116 cells were treated with imidazolones **7e** and **7f** for 24 h at their IC_{50} concentration, and then cells were washed twice with ice-cold phosphate buffered saline (PBS). Subsequently, the treated cells were collected by centrifugation, fixed in ice-cold 70% (*v/v*) ethanol, washed with PBS, re-suspended with 100 µg/mL RNase, stained with 40 µg/mL PI, and analyzed by flow cytometry using FACS Calibur (Becton Dickinson, BD, USA). The cell cycle distributions were calculated using CellQuest software 5.1 (Becton Dickinson) [49,50].

4.2.5. Annexin V-FITC apoptosis assay

Phosphatidylserine externalization was assayed using Annexin V-FITC/PI apoptosis detection kit (BD Biosciences, USA) according to the manufacturer's instructions, as reported earlier [51,52].

4.2.6. Molecular docking simulation

The crystal structure of hCA II (PDB 5LJT [33]) and hCA IX (PDB 5FL4 [34]) were prepared using the Protein Preparation Wizard tool implemented in Maestro - Schrödinger suite, assigning bond orders, adding hydrogens, deleting water molecules, and optimizing H-bonding networks [53]. Energy minimization protocol with a root mean square deviation (RMSD) value of 0.30 was applied using an Optimized Potentials for Liquid Simulation (OPLS3) force field. For the simulations with sulfonate derivatives, 5JLT and 5FL4 were prepared adding the zinc-bound water molecule as fourth ligand of the metal tetrahedral coordination sphere. 3D ligand structures were prepared by Maestro [53]a and evaluated for their ionization states at pH 7.4 ± 0.5 with Epik [53]b. OPLS3 force field in Macromodel [53]e was used for energy minimization for a maximum number of 2500 conjugate gradient iteration and setting a convergence criterion of 0.05 kcal mol^{-1} $Å^{-1}$. The docking grid was centered on the center of mass of the co-crystallized ligands and Glide used with default settings. Ligands were docked with the standard precision mode (SP) of Glide [53]f and the best 5 poses of each molecule retained as output. The best pose for each compound, evaluated in terms of coordination, hydrogen bond interactions and hydrophobic contacts, was refined with Prime [53]d with a VSGB solvatation model considering the target flexible within 3 Å around the ligand [54–56].

Acknowledgements

The authors would like to extend their sincere appreciation to the Deanship of Scientific Research at King Saud University for its funding of this research through the Research Group Project no. RG-1439-65.

Appendix A. Supplementary material

Supplementary data to this article can be found online at https://doi.org/10.1016/j.bioorg.2019.103102.

References

[1] C.T. Supuran, Carbonic anhydrases: from biomedical applications of the inhibitors and activators to biotechnological use for CO2 capture, Taylor & Francis, (2013).
[2] C.T. Supuran, Carbonic anhydrases: novel therapeutic applications for inhibitors and activators, Nat. Rev. Drug Discov. 7 (2008) 168–181.
[3] C. Capasso, C.T. Supuran, Sulfa and trimethoprim-like drugs–antimetabolites acting as carbonic anhydrase, dihydropteroate synthase and dihydrofolate reductase inhibitors, J. Enzyme Inhib. Med. Chem. 29 (2014) 379–387.
[4] C.T. Supuran, Advances in structure-based drug discovery of carbonic anhydrase inhibitors, Expert Opin. Drug Discov. 12 (2017) 61–88.
[5] C.T. Supuran, How many carbonic anhydrase inhibition mechanisms exist? J. Enzyme Inhib. Med. Chem. 31 (2016) 345–360.
[6] D. Neri, C.T. Supuran, Interfering with pH regulation in tumours as a therapeutic strategy, Nat. Rev. Drug Discov. 10 (2011) 767–777.
[7] C.T. Supuran, Carbon-versus sulphur-based zinc binding groups for carbonic anhydrase inhibitors? J. Enzyme Inhib. Med. Chem. 33 (2018) 485–495.
[8] V. Alterio, A. Di Fiore, K. D'Ambrosio, C.T. Supuran, G. De Simone, Multiple binding modes of inhibitors to carbonic anhydrases: how to design specific drugs targeting 15 different isoforms? Chem. Rev. 112 (2012) 4421–4468.
[9] G. De Simone, C.T. Supuran, Carbonic anhydrase IX: Biochemical and crystallographic characterization of a novel antitumor target, Biochim. Biophys. Acta 2010 (1804) 404–409.
[10] J. Pastorek, S. Pastorekova, Hypoxia-induced carbonic anhydrase IX as a target for cancer therapy: from biology to clinical use, Seminars in Cancer Biology, Elsevier, 2015, pp. 52–64.
[11] Y. Lou, P.C. McDonald, A. Oloumi, S. Chia, C. Ostlund, A. Ahmadi, A. Kyle, U. Auf dem Keller, S. Leung, D. Huntsman, B. Clarke, B.W. Sutherland, D. Waterhouse, M. Bally, C. Roskelley, C.M. Overall, A. Minchinton, F. Pacchiano, F. Carta, A. Scozzafava, N. Touisni, J.Y. Winum, C.T. Supuran, S. Dedhar, Targeting tumor hypoxia: suppression of breast tumor growth and metastasis by novel carbonic anhydrase IX inhibitors, Cancer Res. 71 (2011) 3364–3376.
[12] F. Pacchiano, F. Carta, P.C. McDonald, Y. Lou, D. Vullo, A. Scozzafava, S. Dedhar, C.T. Supuran, Ureido-substituted benzenesulfonamides potently inhibit carbonic anhydrase IX and show antimetastatic activity in a model of breast cancer metastasis, J. Med. Chem. 54 (2011) 1896–1902.
[13] C. Congiu, V. Onnis, G. Balboni, C.T. Supuran, Synthesis and carbonic anhydrase I, II, IX and XII inhibition studies of 4-N, N-disubstituted sulfanilamides incorporating 4, 4, 4-trifluoro-3-oxo-but-1-enyl, phenacylthiourea and imidazol-2 (3H)-one/thione moieties, Bioorg. Med. Chem. Lett. 24 (2014) 1776–1779.
[14] F.M. Awadallah, T.A. El-Waei, M.M. Hanna, S.E. Abbas, M. Ceruso, B.E. Oz, O.O. Guler, C.T. Supuran, Synthesis, carbonic anhydrase inhibition and cytotoxic activity of novel chromone-based sulfonamide derivatives, Eur. J. Med. Chem. 96 (2015) 425–435.
[15] F.M. Awadallah, S. Bua, W.R. Mahmoud, H.H. Nada, A. Nocentini, C.T. Supuran, Inhibition studies on a panel of human carbonic anhydrases with N 1-substituted secondary sulfonamides incorporating thiazolinone or imidazolone-indole tails, J. Enzym. Inhib. Med. Chem. 33 (2018) 629–638.
[16] N.M. Abdel Gawad, N.H. Amin, M.T. Elsaadi, F.M.M. Mohamed, A. Angeli, V. De Luca, C. Capasso, C.T. Supuran, Synthesis of 4-(thiazol-2-ylamino)-benzenesulfonamides with carbonic anhydrase I, II and IX inhibitory activity and cytotoxic effects against breast cancer cell lines, Bioorg. Med. Chem. 24 (2016) 3043–3051.
[17] H.H. Georgey, F.M. Manhi, W.R. Mahmoud, N.A. Mohamed, E. Berrino, C.T. Supuran, 1,2,4-Trisubstituted imidazolinones with dual carbonic anhydrase and p38 mitogen-activated protein kinase inhibitory activity, Bioorg. Chem. 82 (2019) 109–116.
[18] W.M. Eldehna, M.F. Abo-Ashour, A. Nocentini, R.S. El-Haggar, S. Bua, A. Bonardi, S.T. Al-Rashood, G.S. Hassan, P. Gratteri, H.A. Abdel-Aziz, Enhancement of the tail hydrophobic interactions within the carbonic anhydrase IX active site via structural extension: design and synthesis of novel *N*-substituted isatins-SLC-0111 hybrids as carbonic anhydrase inhibitors and antitumor agents, Eur. J. Med. Chem. 162 (2019) 147–160.
[19] W.M. Eldehna, A. Nocentini, S.T. Al-Rashood, G.S. Hassan, H.M. Alkahtani, A.A. Almehizia, A.M. Reda, H.A. Abdel-Aziz, C.T. Supuran, Tumor-associated carbonic anhydrase isoform IX and XII inhibitory properties of certain isatin-bearing sulfonamides endowed with *in vitro* anticancer activity towards colon cancer, Bioorg. Med. Chem. 81 (2018) 425–432.
[20] W.M. Eldehna, M.F. Abo-Ashour, A. Nocentini, P. Gratteri, H.I. Eissa, M. Fares, O.E. Ismael, H.A. Ghabbour, M.M. Elaasser, H.A. Abdel-Aziz, C.T. Supuran, Novel 4/3-((4-oxo-5-(2-oxoindolin-3-ylidene) thiazolidin-2-ylidene) amino) benzenesulfonamides: synthesis, carbonic anhydrase inhibitory activity, anticancer activity and molecular modelling studies, Eur. J. Med. Chem. 139 (2017) 250–262.
[21] A.W. Ingersoll, S.H. Babcock, Hippuric acid, Org. Synth. (1932) 40.
[22] E.E. Jun, Ueber die Condensation der Hippursäure mit Phtalsäureanhydrid und mit Benzaldehyd, Justus Liebigs Annalen der Chemie 275 (1) (1893) 1–8.
[23] R.M. Acheson, D.A. Booth, R. Brettle, A.M. Harris, 694. The synthesis of some acylglycines and related oxazolones, J. Chem. Soc. (Resumed) (1960) 3457–3461.
[24] T. Cleary, T. Rawalpally, N. Kennedy, F. Chavez, Catalyzing the Erlenmeyer Plöchl reaction: organic bases versus sodium acetate, Tetrahedron Lett. 51 (2010) 1533–1536.
[25] R.G. Khalifah, The carbon dioxide hydration activity of carbonic anhydrase I. Stop-flow kinetic studies on the native human isoenzymes B and C, J. Biol. Chem. 246 (1971) 2561–2573.
[26] P. Skehan, R. Storeng, D. Scudiero, A. Monks, J. McMahon, D. Vistica, J.T. Warren, H. Bokesch, S. Kenney, M.R. Boyd, New colorimetric cytotoxicity assay for anticancer-drug screening, J. Natl. Cancer Inst. 82 (1990) 1107–1112.
[27] W.M. Eldehna, M. Fares, H.S. Ibrahim, M.A. Alsherbiny, M.H. Aly, H.A. Ghabbour, H.A. Abdel-Aziz, Synthesis and cytotoxic activity of biphenylurea derivatives containing indolin-2-one moieties, Molecules 21 (2016) 762.
[28] W.M. Eldehna, A.M. El Kerdawy, G.H. Al-Ansary, S.T. Al-Rashood, M.M. Ali, A.E. Mahmoud, Type IIA - Type IIB protein tyrosine kinase inhibitors hybridization as an efficient approach for potent multikinase inhibitor development: design, synthesis, anti-proliferative activity, multikinase inhibitory activity and molecular modeling of novel indolinone-based ureides and amides, Eur. J. Med. Chem. 163 (2019) 37–53.
[29] C. Trastour, E. Benizri, F. Ettore, A. Ramaioli, E. Chamorey, J. Pouyssegur, E. Berra, HIF-1alpha and CA IX staining in invasive breast carcinomas: prognosis and treatment outcome, Int. J. Cancer. 120 (2007) 1451–1458.
[30] A.M. Alafeefy, R. Ahmad, M. Abdulla, W.M. Eldehna, A.M.S. Al-Tamimi, H.A. Abdel-Aziz, O. Al-Obaid, F. Carta, A.A. Al-Kahtani, C.T. Supuran, Development of certain new 2-substituted-quinazolin-4-yl-aminobenzenesulfonamide as potential antitumor agents, Eur. J. Med. Chem. 109 (2016) 247–253.
[31] E. Korkeila, K. Talvinen, P.M. Jaakkola, H. Minn, K. Syrjänen, J. Sundström, S. Pyrhönen, Expression of carbonic anhydrase IX suggests poor outcome in rectal cancer, Br. J. Cancer. 100 (2009) 874–880.
[32] T. Mosmann, Rapid colorimetric assay for cellular growth and survival: application to proliferation and cytotoxicity assays, J. Immunol. Methods 65 (1983) 55–63.
[33] A. Nocentini, M. Ferraroni, F. Carta, M. Ceruso, P. Gratteri, C. Lanzi, E. Masini, C.T. Supuran, Benzenesulfonamides incorporating flexible triazole moieties are highly effective carbonic anhydrase inhibitors: synthesis and kinetic, crystallographic, computational, and intraocular pressure lowering investigations, J. Med. Chem. 59 (2016) 10692–10704.
[34] J. Leitans, A. Kazaks, A. Balode, J. Ivanova, R. Zalubovskis, C.T. Supuran, K. Tars, Efficient expression and crystallization system of cancer-associated carbonic anhydrase isoform IX, J. Med. Chem. 58 (2015) 9004–9009.
[35] P.A. Conway, K. Devine, F. Paradisi, A simple and efficient method for the synthesis of Erlenmeyer azlactones, Tetrahedron 65 (2009) 2935–2938.
[36] M. Parveen, A. Ali, S. Ahmed, A.M. Malla, M. Alam, P.S.P. Silva, M.R. Silva, D.-U. Lee, Synthesis, bioassay, crystal structure and ab initio studies of Erlenmeyer azlactones, Spectrochim. Acta A Mol. Biomol. Spectrosc. 104 (2013) 538–545.
[37] M.F. Abo-Ashour, W.M. Eldehna, A. Nocentini, H.S. Ibrahim, S. Bua, H.A. Abdel-Aziz, S.M. Abou-Seri, C.T. Supuran, Novel synthesized SLC-0111 thiazole and thiadiazole analogues: determination of their carbonic anhydrase inhibitory activity and molecular modeling studies, Bioorg. Chem. 87 (2019) 794–802.
[38] W.M. Eldehna, M.F. Abo-Ashour, E. Berrino, D. Vullo, H.A. Ghabbour, S.T. Al-

Rashood, G.S. Hassan, H.M. Alkahtani, A.A. Almehizia, A. Alharbi, SLC-0111 enaminone analogues, 3/4-(3-aryl-3-oxopropenyl) aminobenzenesulfonamides, as novel selective subnanomolar inhibitors of the tumor-associated carbonic anhydrase isoform IX, Bioorg. Chem. 83 (2019) 549–558.
[39] H.S. Ibrahim, H.A. Allam, W.R. Mahmoud, A. Bonardi, A. Nocentini, P. Gratteri, E.S. Ibrahim, H.A. Abdel-Aziz, C.T. Supuran, Dual-tail arylsulfone-based benzenesulfonamides differently match the hydrophobic and hydrophilic halves of human carbonic anhydrases active sites: Selective inhibitors for the tumor-associated hCA IX isoform, Eur. J. Med. Chem. 152 (2018) 1–9.
[40] M.F. Abo-Ashour, W.M. Eldehna, A. Nocentini, H.S. Ibrahim, S. Bua, S.M. Abou-Seri, C.T. Supuran, Novel hydrazido benzenesulfonamides-isatin conjugates: Synthesis, carbonic anhydrase inhibitory activity and molecular modeling studies, Eur. J. Med. Chem. 157 (2018) 28–36.
[41] M. Fares, R.A. Eladwy, A. Nocentini, S.R.A. El Hadi, H.A. Ghabbour, A. Abdel-Megeed, W.M. Eldehna, H.A. Abdel-Aziz, C.T. Supuran, Synthesis of bulky-tailed sulfonamides incorporating pyrido [2, 3-d][1, 2, 4] triazolo [4, 3-a] pyrimidin-1 (5H)-yl) moieties and evaluation of their carbonic anhydrases I, II, IV and IX inhibitory effects, Bioorg. Med. Chem. 25 (2017) 2210–2217.
[42] A. Monks, D. Scudiero, P. Skehan, R. Shoemaker, K. Paull, D. Vistica, C. Hose, J. Langley, P. Cronise, A. Vaigro-Wolfe, M. Gray-Goodrich, H. Campbell, M.R. Boyd, Feasibility of a high-flux anticancer drug screen using a diverse panel of cultured human tumor cell lines, J. Natl. Cancer Inst. 83 (1991) 757–766.
[43] M.R. Boyd, K.D. Paull, Some practical considerations and applications of the national cancer institute in vitro anticancer drug discovery screen, Drug Dev. Res. 34 (1995) 91–109.
[44] M.R. Boyd, in: B.A. Teicher (Ed.), Cancer Drug Discovery and Development: Anticancer Drug Development Guide: Preclinical Screening, Clinical Trials and Approval, second ed., Humana Press, Totowa, NJ, USA, 2014, pp. 41-62 (Chapter 1).
[45] M.F. Abo-Ashour, W.M. Eldehna, R.F. George, M.M. Abdel-Aziz, M.M. Elaasser, N.M. Abdel Gawad, A. Gupta, S. Bhakta, S.M. Abou-Seri, Novel indole-thiazolidinone conjugates: design, synthesis and whole-cell phenotypic evaluation as a novel class of antimicrobial agents, Eur. J. Med. Chem. 160 (2018) 49–60.
[46] W.M. Eldehna, G.S. Hassan, S.T. Al-Rashood, T. Al-Warhi, A.E. Altyar, H.M. Alkahtani, A.A. Almehizia, H.A. Abdel-Aziz, Synthesis and in vitro anticancer activity of certain novel 1-(2-methyl-6-arylpyridin-3-yl)-3-phenylureas as apoptosis-inducing agents, J. Enzym. Inhib. Med. Chem. 34 (2019) 322–332.
[47] R.S.M. Ismail, S.M. Abou-Seri, W.M. Eldehna, N.S.M. Ismail, S.M. Elgazwi, H.A. Ghabbour, Mahmoud Salama Ahmed, F.T. Halaweish, D.A. Abou El Ella, Novel series of 6-(2-substitutedacetamido)-4-anilinoquinazolines as EGFR-ERK signal transduction inhibitors in MCF-7 breast cancer cells, Eur. J. Med. Chem. 155 (2018) 782–796.
[48] H. Almahli, E. Hadchity, M.Y. Jaballah, R. Daher, H.A. Ghabbour, M.M. Kabil, N.S. Al-shakliah, W.M. Eldehna, Development of novel synthesized phthalazinone-based PARP-1 inhibitors with apoptosis inducing mechanism in lung cancer, Bioorg. Chem. 77 (2018) 443–456.
[49] W.M. Eldehna, D.H. EL-Naggar, A.R. Hamed, H.S. Ibrahim, H.A. Ghabbour, H.A. Abdel-Aziz, One-pot three-component synthesis of novel spirooxindoles with potential cytotoxic activity against triple-negative breast cancer MDAMB-231 cells, J. Enzym. Inhib. Med. Chem. 33 (2018) 309–318.
[50] A. Sabt, O.M. Abdelhafez, R.S. El-Haggar, H.M.F. Madkour, W.M. Eldehna, E.E.A.M. El-Khrisy, M.A. Abdel-Rahman, L.A. Rashed, Novel coumarin-6-sulfonamides as apoptotic anti-proliferative agents: synthesis, in vitro biological evaluation, and QSAR studies, J. Enzym. Inhib. Med. Chem. 33 (2018) 1095–1107.
[51] W.M. Eldehna, M.F. Abo-Ashour, H.S. Ibrahim, G.H. Al-Ansary, H.A. Ghabbour, M.M. Elaasser, H.Y.A. Ahmed, N.A. Safwat, Novel [(3-indolylmethylene) hydrazono] indolin-2-ones as apoptotic anti-proliferative agents: design, synthesis and in vitro biological evaluation, J. Enzym. Inhib. Med. Chem. 33 (2018) 686–700.
[52] W.M. Eldehna, H. Almahli, G.H. Al-Ansary, H.A. Ghabbour, M.H. Aly, O.E. Ismael, A. Al-Dhfyan, H.A. Abdel-Aziz, Synthesis and in vitro anti-proliferative activity of some novel isatins conjugated with quinazoline/phthalazine hydrazines against triple-negative breast cancer MDA-MB-231 cells as apoptosis-inducing agents, J. Enzym Inhib. Med. Chem. 32 (2017) 600–613.
[53] Schrödinger Suite Release 2018-2, Schrödinger, LLC, New York, NY, 2018: (a) Maestrov.11.6; (b) Epik, v.4.4; (c) Impact, v.7.9; (d) Prime, v.5.2; (e) Macromodel v.12.0. (f) Glide, v.7.9.
[54] A. Nocentini, P. Gratteri, C.T. Supuran, Phosphorus versus sulfur: discovery of benzenephosphonamidates as versatile sulfonamide-mimic chemotypes acting as carbonic anhydrase inhibitors, Chemistry. 25 (2019) 1188–1192.
[55] A. Nocentini, A. Bonardi, P. Gratteri, B. Cerra, A. Gioiello, Supuran CT steroids interfere with human carbonic anhydrase activity by using alternative binding mechanisms, J. Enzyme Inhib. Med. Chem. 33 (2018) 1453–1459.
[56] A. Nocentini, F. Carta, M. Tanc, S. Selleri, C.T. Supuran, C. Bazzicalupi, P. Gratteri, Deciphering the mechanism of human carbonic anhydrases inhibition with sulfocoumarins: computational and experimental studies, Chemistry 24 (2018) 7840–7844.